Quantum turbulence by vortex stirring in a spinor Bose-Einstein condensate

B. Villaseñor, R. Zamora-Zamora, D. Bernal, and V. Romero-Rochín*

Instituto de Física, Universidad Nacional Autónoma de México, Apartado Postal 20-364, 01000 México Distrito Federal, Mexico

(Received 6 September 2013; published 10 March 2014)

We introduce a mechanism to develop a turbulent flow in a spinor Bose-Einstein condensate, consisting in the stirring of a single line vortex by means of an external magnetic field. We find that density and velocity fluctuations have white-noise power spectra at large frequencies and that the energy spectrum obeys Kolmogorov 5/3 law in the turbulent region. As the stirring is turned off, the flow decays to an agitated nonequilibrium state that shows an energy bottleneck crossover at small length scales. We demonstrate our findings by numerically solving two-state spinor coupled three-dimensional Gross-Pitaevskii equations. We suggest that this mechanism may be experimentally implemented in spinor ultracold gases confined by optical traps.

DOI: 10.1103/PhysRevA.89.033611 PACS number(s): 67.85.De, 67.25.dk, 67.85.Fg

Ever since Kolmogorov's seminal ideas on classical turbulence [1], stochastic and universal laws have been sought for and discovered to be obeyed by highly complex fluid flows. Among the most celebrated predictions is the so-called "5/3" energy cascade. Although turbulence has remained as a fascinating topic of study classically [2] and in helium superfluids [3,4], there has been great interest in the study of turbulence in ultracold superfluid gases (see Refs. [5–7] for recent reviews). Of noteworthy relevance are the experimental realizations of quantum turbulence (QT) in a ^{87}Rb ultracold gas in a magnetic trap [8], and in a two-dimensional version confined by an annular trap [9]. On the theoretical side, much effort has been devoted to understand QT as a "vortex tangle" as well as its velocity statistics [10–14].

Following Ref. [15], where it was shown that Gross-Pitaevskii (GP) spinor Bose-Einstein condensates (SBEC) in optical traps can support vortices "on demand" in the presence of external magnetic fields, we study here the dynamics generated by the simple stirring of a single vortex in a three-dimensional (3D), spin 1/2, SBEC. We find that even for mild stirrings a turbulent flow is developed in both components of SBEC. Because GP superfluids lack a dissipative mechanism it is difficult to produce a true turbulent steady state, yet a turbulent phase is clearly obtained during and after the stirring process. When the latter is turned off, the flow decays to a nonequilibrium stationary state with turbulence remnants and an energy bottleneck contribution at small length scales [16]. There have been other proposals for the creation of QT, either by starting in a nonequilibrium state [17] or by rotating a BEC cloud [10,18], all of them in a one-component BEC cloud. Ours requires a multicomponent spinor BEC.

The problem reduces to finding the solution of the following GP equations describing a 3D $s = 1/2$ SBEC,

$$\left[-\frac{\hbar^2}{2m}\nabla^2 + \frac{1}{2}m\omega^2 r^2 + g(|\psi_+|^2 + |\psi_-|^2) - m_0 B_x \sigma_x - m_0 B_y \sigma_y - i\hbar\frac{\partial}{\partial t}\right]\begin{pmatrix}\psi_+\\ \psi_-\end{pmatrix} = 0. \quad (1)$$

We solve these equations in a 128^3 grid using finite differences and Runge-Kutta methods. Calculations were performed in a 530-core C2075 Tesla GPU using PY-CUDA. Computational details may be found in the Supplemental Material [19]. The SBEC is confined by an isotropic harmonic trap of frequency ω, with contact interactions independent of the spinor component $g = 4\pi\hbar^2 aN/m$, where a is the common scattering length and N is the number of atoms. σ_x and σ_y are Pauli matrices and m_0 is the atom magnetic moment. In units $\hbar = m = \omega = 1$, we use $g = 8000$; this may represent $N = 10^5$ ^{87}Rb atoms, with $a = 50$ Å, confined in a dipolar optical trap with $\omega = (2\pi)100$ Hz. These data are close to the values of the hyperfine states $F = 1$, $m_F = -1$ and $F = 2$, $m_F = 2$ in ^{87}Rb [20]. A time unit corresponds to 1.6 ms approximately. We consider the magnetic field as

$$m_0 B_x = \kappa x, \quad m_0 B_y = -\kappa\,(y - y_0 \sin\,\Omega t)\,, \quad (2)$$

where y_0 and Ω are the amplitude and frequency of the excitation. We use $\kappa = 1.0$; this choice for ^{87}Rb and the optical trap mentioned above, corresponds to a magnetic field gradient of about 1 G/cm, a value within current experimental reach.

Initially, for times $t \leqslant 0$, $y_0 = 0$ and the system is in its stationary ground state, $\psi_\alpha(\vec{r},t) = e^{-i\mu t/\hbar}\psi_\alpha^0(\vec{r})$, where $\mu \approx 15.5$ is the chemical potential and $\psi_\alpha^0(\vec{r})$ is a solution with a single vortex line of charge $+1$ in the $\alpha = +$ component at $x = y = 0$, and with a density spike for $\alpha = -$ [15]. One can check that the expectation value of angular momentum is different from zero only in the z direction of component $\alpha = +$. Figure 1 shows density plots of this vortex solution. By writing $\phi_\alpha = |\psi_\alpha| e^{i\phi_\alpha}$, the density and velocity fields are given by $\rho_\alpha = |\psi_\alpha|^2$ and $\vec{v}_\alpha = \hbar\nabla\phi_\alpha/m$ [21].

At $t = 0$ the excitation is turned on, $y_0 \neq 0$ in Eq. (2), which makes the line with zero magnetic field oscillate along the y direction with amplitude y_0 and frequency Ω. The ensuing superfluid flow behavior is quite complex depending on the values of y_0 and Ω and on the time the oscillation is maintained. An extensive study of these variables yields threshold values of y_0 and Ω, above which, a turbulent flow pattern appears. We also find that angular momentum is excited in all spatial and spinor components. For present purposes, we have chosen $y_0 = 1.0$, about 1/7 the Thomas-Fermi radius of the condensate, and $\Omega = 0.5\omega$, hence avoiding resonances of collective motions [22].

Three excitations are studied: (I) the excitation never stops; (II) the excitation runs for a time $\tau_e = 5(2\pi)/\Omega$, then the

*romero@fisica.unam.mx

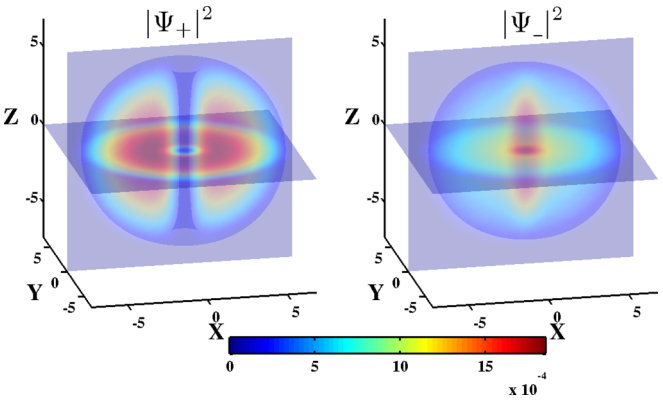

FIG. 1. (Color online) Density plots of the initial state. Component $\alpha = +$ shows a line vortex, charge $+1$, while $\alpha = -$ presents a density spike.

external magnetic field is ramped down, $\kappa \to 0$, linearly in a time $0.4\tau_e$; and (III) the excitation runs for τ_e; the field returns to its initial value but it is never turned off. Due to the lack of energy dissipation, the excitation injects energy into the system and remains there. In (I) energy is kept entering the system, while in the others, energy is only received by the system during the excitation time. The energy is given by

$$E = \int \left(-\frac{\hbar^2}{2m}\psi_\alpha^* \nabla^2 \psi_\alpha + V_{\text{ext}}\psi_\alpha^*\psi_\alpha - m_0 \psi_\alpha^* [\vec{B}\cdot\vec{\sigma}]^{\alpha\beta}\psi_\beta + \frac{g}{2}\psi_\beta^*\psi_\beta\psi_\alpha^*\psi_\alpha \right) d^3r, \quad (3)$$

with summation over repeated indices. In (II) and (III) the energy is constant after the excitation and the system reaches a nonequilibrium stationary state. We determine such a stationary state by monitoring the total average angular momentum, which tends to a stable value after a time of the order of $2\tau_e$. Below, we analyze statistical properties of the stationary state.

Figure 2 shows snapshots of the velocity field evolution during the excitation time $0 \leqslant t \leqslant \tau_e$. One observes that the superfluid flow cannot follow the motion of the magnetic field, creating a complicated pattern of line and ring vortices. First, the line vortex at component $+$ bends, while another one is nucleated in component $-$. Then, vortices are created in pairs, one in component $+$ and another in the other component, with two types, vortex rings and line vortices, that end at the surface of the cloud. Because vortices nucleate, move and disperse, and dissipate at the surface of the cloud, it is difficult to quantify the total circulation. Since the fluid is compressible, Kelvin waves and phonon excitations are generated creating bursts in the velocity field. Full videos of these figures are shown in the Supplemental Material [19].

Figure 3 shows snapshots of cases (II) and (III), at a time later than the excitation time $t \gg \tau_e$ (see Supplemental Material [19] for full videos). In (II), while there is no magnetic field in the steady state, the flow remains agitated due to the lack of dissipation. Case (III) is particularly interesting showing a stationary semiturbulent state with two additional line vortices in each component, all of them with topological charge -1, in addition to the original vortex at the origin with charge $+1$. The additional vortices orbit around the original vortex with different angular velocities. In (I), where the excitation never stops, the noteworthy aspect is that, while vortices and phonons keep being excited, the velocity fields acquire maximum values at the edge of the clouds.

The statistical properties of the stationary state in (II) and (III) are calculated as follows. First, after $t = \tau_e$, we let the system evolve until the total angular momentum decays to an almost constant value, signaling a "stationary" state; this time is of the order of $2.0\tau_e$. Then, the system evolves for another long interval of time, of order $6.5\tau_e$, during which we calculate the time average of the density and velocity fields and their fluctuations; namely,

$$\begin{aligned} \rho_\alpha(\vec{r},t) &= \rho_\alpha^s(\vec{r}) + \delta\rho_\alpha(\vec{r},t), \\ \vec{v}_\alpha(\vec{r},t) &= \vec{v}_\alpha^s(\vec{r}) + \delta\vec{v}_\alpha(\vec{r},t), \end{aligned} \quad (4)$$

where superscript "s" denotes the time average of the quantity in question. Barring low-frequency collective modes, the fluctuating part should capture the expected universal and homogeneous turbulent contribution. Figure 4 shows the power spectrum of the fluctuating parts $|\widetilde{\delta\rho}_\alpha(\vec{r},\omega)|^2$ and $|\widetilde{\delta\vec{v}}_\alpha(\vec{r},\omega)|^2$ for the $+$ spin component of (II) and (III), in two different spatial regions: one in the vicinity of the position of the original line vortex, the other near the edge of the cloud. The most relevant result is that, the farther the spatial point is from the initial vortex region, the power spectra is essentially white noise. Near the vortex region the spectra shows both white noise in the ultraviolet region, while some kind of $1/f^\beta$

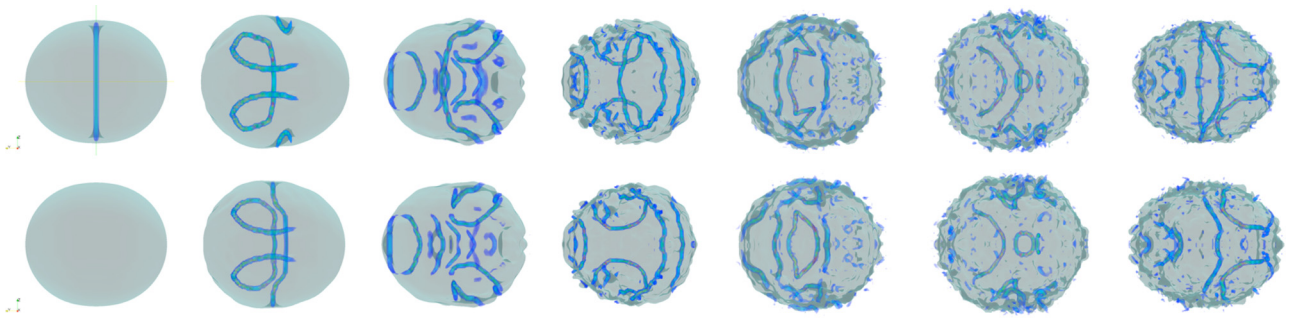

FIG. 2. (Color online) Time evolution of velocity fields of both spinorial components during excitation time $0 \leqslant t \leqslant \tau_e$, with $\tau = 5(2\pi)/\Omega$. The upper row corresponds to component $\alpha = +$, and the lower one to $\alpha = -$. The snapshots are at times $t_n = 0,1,\ldots,6,(\tau_e/6)$. We use dimensionless units $\hbar = m = \omega = 1$ (see Supplemental Material [19] for a full video).

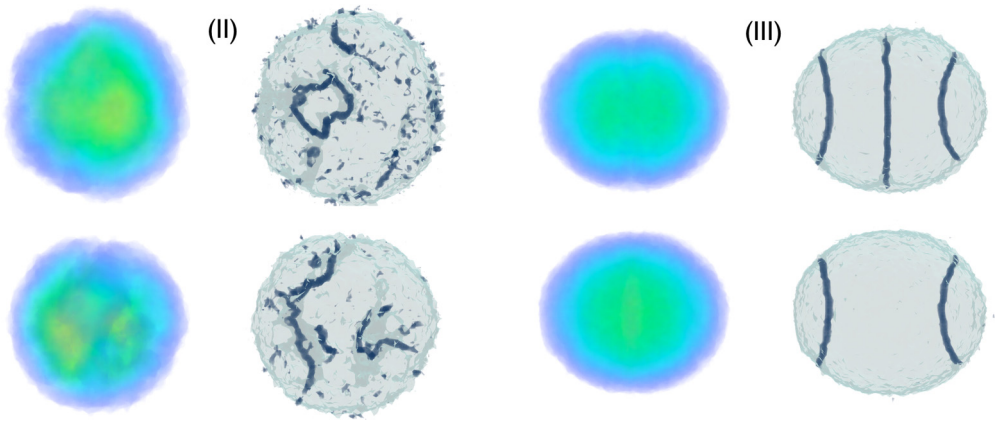

FIG. 3. (Color online) Density and velocity fields after stirring is turned off. The upper row is component $\alpha = +$, and the lower one $\alpha = -$. (II) External magnetic field is ramped out; the snapshot is at $t = 245$. (III) Magnetic field is kept on; te snapshot is at $t = 366$. We use dimensionless units $\hbar = m = \omega = 1$ (see Supplemental Material [19] for full videos).

noise in the low-frequency region, β ranging from 0 to 2.5. This behavior may be "contaminated" from low-frequency collective modes that cannot be completely removed with the time average. In (III) the large peaks at low frequencies correspond to the orbiting motion of the stable vortices (see Fig. 2). The white-noise fluctuating contribution may be identified as the remnants of the turbulent component of the flow.

The second analysis concerns the wave-number dependence of the incompressible part of the kinetic energy. It is believed [4–7] that in the turbulent region it should show Kolmogorov "5/3" law [1], indicating an energy cascade from large to small length scales. This is also true in wave turbulence [23]. Since GP superfluid flow has both compressible and incompressible contributions, it has been argued [24] that the incompressible part of the kinetic energy should show Kolmogorov cascade. This decomposition is achieved by separating the divergenceless and curless parts of the vector $\sqrt{\rho_\alpha}\vec{v}_\alpha$ for both spin components. The divergenceless part yields the incompressible contribution to the kinetic energy K_i,

$$K_i^\alpha = \int \frac{1}{2}\left(\rho_\alpha \vec{v}_\alpha^2\right)_i d^3r = \int \epsilon_i^\alpha(k)dk, \qquad (5)$$

where $k = |\vec{k}|$. The expected Kolmogorov law is $\epsilon_i^\alpha(k) \sim k^{-5/3}$ in an intermediate range of k, corresponding to length scales $l < \lambda < a$, with l and a of the order of the sizes of the cloud and of the vortices core. Figure 5 shows $\epsilon_i^+(k)$ for cases (I)–(III), for several times. One observes that the curve shape is reminiscent of the typical ones of classical turbulence [2] for small $k \lesssim l^{-1}$, followed by a region that obeys Kolmogorov law, but then it differs from the classical one in the tail $k \sim a^{-1}$. In classical turbulence the curve bends down since viscosity plays its role dissipating energy into heat. Here, we find that the curve bends up for long k, as $\epsilon(k) \sim k^2$, a free particlelike spectrum. This has an explanation. It is clear that a cascade is present: Energy enters the system through the stirring of the initial line vortex, creating in turn smaller vortices and other compressible excitations as phonons, transferring energy to smaller length scales. But since GP does not have a mechanism to dissipate heat into a thermal cloud, energy tends to be concentrated at high-k excitations. This leads to a state of quasiequilibrium with a kind of energy equipartition yielding the k^2 dependence, similarly to the bottleneck phenomenon expected in Kelvin -wave turbulence [16]. Recalling that as time passes by most of the large fluctuations occur at the edges of the clouds (see the videos in the Supplemental Material [19])

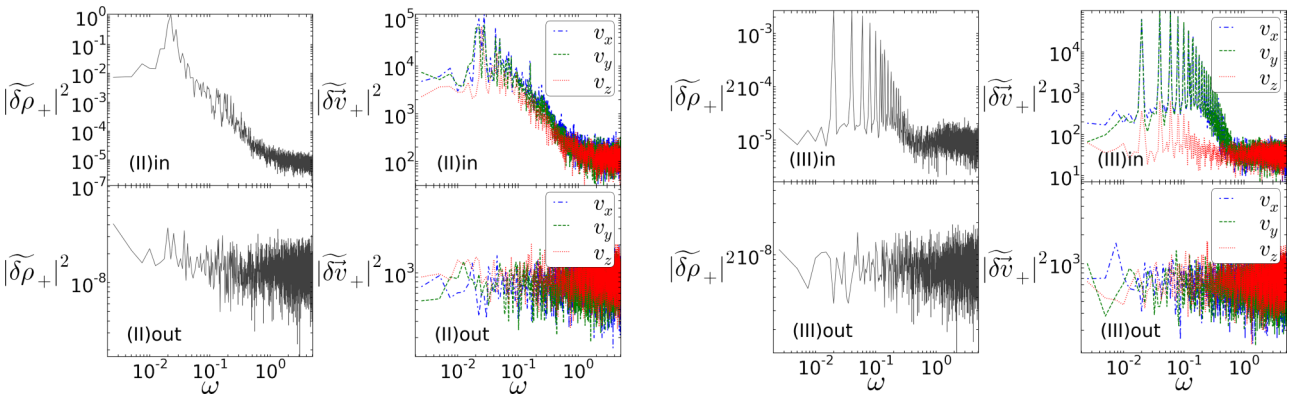

FIG. 4. (Color online) Power spectra $|\delta\widetilde{\rho}_\alpha(\vec{r},\omega)|^2$ and $|\delta\widetilde{\vec{v}}_\alpha(\vec{r},\omega)|^2$, for $\alpha = +$, at nonequilibrium steady state, for two spatial positions of (II) and (III): "in" is near the original vortex and "out" is near the edge of the cloud. We use dimensionless units $\hbar = m = \omega = 1$.

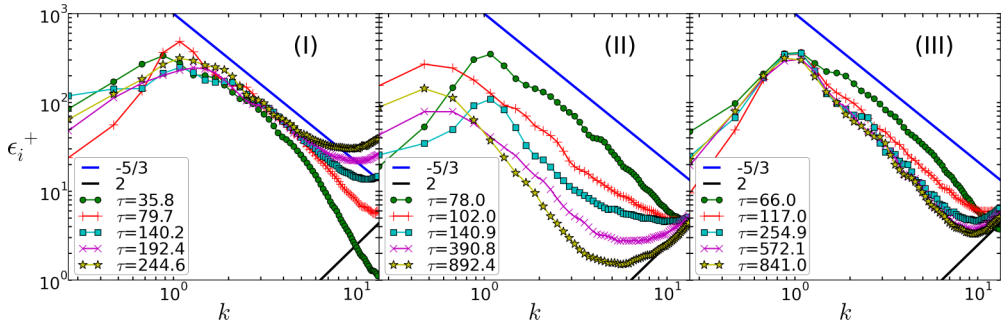

FIG. 5. (Color online) Incompressible kinetic energy ϵ_i^+ vs k for cases (I)–(III), at different times. The blue solid line is at slope $-5/3$; the black solid line is at slope $+2$. We use dimensionless units $\hbar = m = \omega = 1$.

one concludes that the excitations both cascade their energy and migrate it to the outer regions of the cloud. This has a further consequence. In real experimental finite-temperature BEC clouds, the superfluid region is concentrated in the center of the cloud, while the outer region is a thermal shell where viscosity and heat dissipation occur. This part is completely missed by GP. However, our calculations indicate that if the thermal cloud were included, the small length-scale excitations would find their way there and would eventually be dissipated into heat. This would be a turbulence decay mechanism, with a concomitant increase of temperature of the whole BEC cloud. A calculation of this sort may be implemented with the techniques of Refs. [10,25–27]. Regarding Kolmogorov law, we find that it is better obeyed during intermediate times when turbulence occurs, and that for longer times the long-k accumulation tends to bend the curve, deviating it slightly from the $-5/3$ slope. Because our simulated BEC clouds are not very large, this may also be a finite-size effect.

To conclude, we believe this study indicates a feasible and simple way of producing quantum turbulence in ultracold spinorial BEC superfluids. The initial line vortex may be obtained by an arrangement of long wires carrying appropriate electric currents [15], while the stirring may be performed by using ac currents.

We acknowledge support from DGAPA UNAM Grant No. IN108812.

[1] A. N. Kolmogorov, Proc. R. Soc. A **434**, 9 (1991); **434**, 15 (1991).
[2] U. Frisch, *Turbulence. The Legacy of A. N. Kolmogorov* (Cambridge University Press, Cambridge, England, 1995).
[3] W. F. Vinen and J. J. Niemela, J. Low Temp. Phys. **128**, 167 (2002).
[4] W. F. Vinen, J. Low. Temp. Phys. **161**, 419 (2010).
[5] M. S. Paoletti and D. P. Lathrop, Annu. Rev. Condens. Matter. Phys. **2**, 213 (2011).
[6] S. K. Nemirovskii, Phys. Rep. **524**, 85 (2013).
[7] M. Tsubota, J. Low. Temp. Phys. **171**, 571 (2013).
[8] E. A. L. Henn, J. A. Seman, G. Roati, K. M. F. Magalhães, and V. S. Bagnato, Phys. Rev. Lett. **103**, 045301 (2009).
[9] T. W. Neely, A. S. Bradley, E. C. Samson, S. J. Rooney, E. M. Wright, K. J. H. Law, R. Carretero-Gonzalez, P. G. Kevrekidis, M. J. Davis, and B. P. Anderson, Phys. Rev. Lett. **111**, 235301 (2013).
[10] M. Kobayashi and M. Tsubota, Phys. Rev. A **76**, 045603 (2007).
[11] A. C. White, C. F. Barenghi, N. P. Proukakis, A. J. Youd, and D. H. Wacks, Phys. Rev. Lett. **104**, 075301 (2010).
[12] A. C. White, N. P. Proukakis, A. J. Youd, D. H. Wacks, A. W. Baggaley, and C. F. Barenghi, J. Phys. Conf. Proc. **318**, 062003 (2011).
[13] J. A. Seman, E. A. L. Henn, R. F. Shiozaki, G. Roati, F. J. Poveda-Cuevas, K. M. F. Magalhães, V. I. Yukalov, M. Tsubota, M. Kobayashi, K. Kasamatsu, and V. S. Bagnato, Laser Phys. Lett. **8**, 691 (2011).
[14] B. Nowak, J. Schole, D. Sexty, and T. Gasenzer, Phys. Rev. A **85**, 043627 (2012).
[15] R. Zamora-Zamora, M. Lozada-Hidalgo, S. F. Caballero-Benitez, and V. Romero-Rochin, Phys. Rev. A **86**, 053624 (2012).
[16] V. S. L'vov, S. V. Nazarenko, and O. Rudenko, Phys. Rev. B **76**, 024520 (2007).
[17] N. G. Berloff and B. V. Svistunov, Phys. Rev. A **66**, 013603 (2002).
[18] N. G. Parker and C. S. Adams, Phys. Rev. Lett. **95**, 145301 (2005).
[19] See Supplemental Material at http://link.aps.org/supplemental/10.1103/PhysRevA.89.033611 for further explanation of the numerical calculations and for full videos of the time evolution of the density and velocity fields of cases (I), (II), and (III).
[20] M. Egorov, B. Opanchuk, P. Drummond, B. V. Hall, P. Hannaford, and A. I. Sidorov, Phys. Rev. A **87**, 053614 (2013).
[21] E. Yukawa and M. Ueda, Phys. Rev. A **86**, 063614 (2012).
[22] S. Stringari, Phys. Rev. Lett. **77**, 2360 (1996).
[23] L. Boué, R. Dasgupta, J. Laurie, V. L'vov, S. Nazarenko, and I. Procaccia, Phys. Rev. B **84**, 064516 (2011).
[24] C. Nore, M. Abid, and M. E. Brachet, Phys. Fluids **9**, 2644 (1997).
[25] M. Kobayashi and M. Tsubota, Phys. Rev. Lett. **97**, 145301 (2006).
[26] B. Jackson, N. P. Proukakis, C. F. Barenghi, and E. Zaremba, Phys. Rev. A **79**, 053615 (2009).
[27] A. S. Bradley, C. W. Gardiner, and M. J. Davis, Phys. Rev. A **77**, 033616 (2008).